# NAVAL POSTGRADUATE SCHOOL
## Monterey, California

# THESIS

LOCALIZATION OF BURIED OBJECTS IN WATER-SATURATED SAND BY VARIABLE INCIDENCE ACOUSTIC PULSE REFLECTIONS

by

Gwan-Sik Bang

June 1985

Thesis Co-Advisors: Suk Wang Yoon
Thomas B. Gabrielson





Approved for public release; distribution is unlimited

UNCLASSIFIED

SECURITY CLASSIFICATION OF THIS PAGE (When Data Entered)

| REPORT DOCUMENTATION PAGE | | READ INSTRUCTIONS BEFORE COMPLETING FORM |
|---|---|---|
| 1. REPORT NUMBER | 2. GOVT ACCESSION NO. AD-A158 069 | 3. RECIPIENT'S CATALOG NUMBER |
| 4. TITLE (and Subtitle) Localization of Buried Objects in Water-Saturated Sand by Variable Incidence Acoustic Pulse Reflections | | 5. TYPE OF REPORT & PERIOD COVERED Master's Thesis June 1985 |
| | | 6. PERFORMING ORG. REPORT NUMBER |
| 7. AUTHOR(s) Gwan-Sik Bang | | 8. CONTRACT OR GRANT NUMBER(s) |
| 9. PERFORMING ORGANIZATION NAME AND ADDRESS Naval Postgraduate School Monterey, California 93943-5100 | | 10. PROGRAM ELEMENT, PROJECT, TASK AREA & WORK UNIT NUMBERS |
| 11. CONTROLLING OFFICE NAME AND ADDRESS Naval Postgraduate School Monterey, California 93943-5100 | | 12. REPORT DATE June 1985 |
| | | 13. NUMBER OF PAGES 56 |
| 14. MONITORING AGENCY NAME & ADDRESS (if different from Controlling Office) | | 15. SECURITY CLASS. (of this report) Unclassified |
| | | 15a. DECLASSIFICATION/DOWNGRADING SCHEDULE |

16. DISTRIBUTION STATEMENT (of this Report)

Approved for public release; distribution is unlimited

17. DISTRIBUTION STATEMENT (of the abstract entered in Block 20, if different from Report)

18. SUPPLEMENTARY NOTES

19. KEY WORDS (Continue on reverse side if necessary and identify by block number)

$T^2$-$X^2$ Method; Ray Parameter Method, Acoustic Pulse Reflections; Water-Saturated Sand

20. ABSTRACT (Continue on reverse side if necessary and identify by block number)

The purpose of this project is to localize buried objects in water-saturated sand by variable incidence acoustic pulse reflections. In particular, thin aluminum plates are used to model the buried objects. The sound speed and the depth of the overlying sand layer are predicted by using the $T^2$-$X^2$ and the ray parameter methods. The experimentally computed results

DD FORM 1 JAN 73 1473 EDITION OF 1 NOV 65 IS OBSOLETE S/N 0102-LF-014-6601



UNCLASSIFIED

SECURITY CLASSIFICATION OF THIS PAGE (When Data Entered)

#20 - ABSTRACT - (CONTINUED)

have an average 3.5% depth error. The calculated speed of sound in the water-saturated sand layer differed by 8.1% between the $T^2$-$X^2$ and the ray parameter methods.

Approved for public release; distribution is unlimited.

# Localization of Buried Objects in Water-Saturated Sand by Variable Incidence Acoustic Pulse Reflections

by

Gwan-Sik Bang
Major, Republic of Korea Army
B.S., Han Yang University, 1975

Submitted in partial fulfillment of the requirements for the degree of

MASTER OF SCIENCE IN PHYSICS

from the

NAVAL POSTGRADUATE SCHOOL
June 1985



Author: Gwan-Sik Bang
Gwan-Sik Bang

Approved by: Suk Wang Yoon
Suk Wang Yoon, Thesis Advisor

Thomas B. Gabrielson, Co-Advisor

Gordon E. Schacher, Chairman,
Department of Physics

John N. Dyer,
Dean of Science and Engineering

## ABSTRACT

The purpose of this project is to localize buried objects in water-saturated sand by variable incidence acoustic pulse reflections. In particular, thin aluminum plates are used to model the buried objects. The sound speed and the depth of the overlying sand layer are predicted by using the $T^2$-$X^2$ and the ray parameter methods. The experimentally computed results have an average 3.5% depth error. The calculated speed of sound in the water-saturated sand layer differed by 8.1% between the $T^2$-$X^2$ and the ray parameter methods.

TABLE OF CONTENTS


I. INTRODUCTION ---------- 9

A. OBJECTIVES ---------- 9

B. APPROACH ---------- 10

C. BACKGROUND ---------- 10

II. THEORY ---------- 12

A. T-X AND $T^2$-$X^2$ METHODS ---------- 12

B. THE RAY PARAMETER METHOD ---------- 16

III. EXPERIMENTAL PROCEDURES ---------- 21

A. ARRANGEMENT OF THE EXPERIMENT ---------- 21

B. EXPERIMENTAL PROCEDURE ---------- 25

C. SUMMARY OF EXPERIMENTAL PROCEDURE ---------- 30

IV. ANALYSIS AND RESULTS OF EXPERIMENTS ---------- 32

A. MEASUREMENT AND ANALYSIS ---------- 32

1. Measurement 1 ---------- 32

2. Measurement 2 ---------- 35

3. Measurement 3 ---------- 38

4. Measurement 4 ---------- 42

5. Measurement 5 ---------- 45

B. OVERALL RESULTS ---------- 48

V. DISCUSSIONS AND CONCLUSIONS ---------- 50

LIST OF REFERENCES ---------- 54

INITIAL DISTRIBUTION LIST ---------- 55

## LIST OF TABLES


I. Speed of Sound (Measurement 1) ---------- 32

II. Speed of Sound (Measurement 2) ---------- 35

III. Speed of Sound (Measurement 3) ---------- 39

IV. Speed of Sound (Measurement 4) ---------- 42

V. Speed of Sound (Measurement 5) ---------- 45

VI. Summary of Brief Results ---------- 49

VII. The Detailed Results of Total Experiment -------- 51

## LIST OF FIGURES


2.1 Geometry of Layers ---------- 12

2.2 T-X and $T^2$-$X^2$ Curves ---------- 14

2.3 Geometry of Ray Parameter ---------- 17

2.4 T-X Curve and the Ray Parameter ---------- 19

3.1 Block Diagram ---------- 23

3.2 4 Cycle Pulse Signal ---------- 24

3.3 8 Cycle Pulse Signal ---------- 24

3.4 Location of Projector, Hydrophone and Plates ---- 26

3.5 Projector Is Not on the Center Line ---------- 26

3.6 Waves in the Isopseed Shallow Water Channel ----- 27

3.7 Different Kinds of Waves on Oscilloscope -------- 28

4.1 T-X and $T^2$-$X^2$ Plots (Measurement 1) ---------- 34

4.2 T-X and $T^2$-$X^2$ Plots (Measurement 2) ---------- 36

4.3 Measurement 2 at X = 34.5 cm ---------- 37

4.4 Measurement 2 at X = 39.6 cm ---------- 37

4.5 T-X and $T^2$-$X^2$ Plots (Measurement 3) ---------- 40

4.6 Measurement 3 at X = 21.7 cm ---------- 41

4.7 Measurement 3 at X = 29.3 cm ---------- 41

4.8 T-X and $T^2$-$X^2$ Plots (Measurement 4) ---------- 43

4.9 Measurement 4 at X = 35.1 cm ---------- 44

4.10 Measurement 4 at X = 47.7 cm ---------- 44

4.11 T-X and $T^2$-$X^2$ Plots (Measurement 5) ---------- 46

4.12 Measurement 5 at X = 28.2 cm ---------- 47

4.13 Measurement 5 at X = 48.8 cm ---------- 47

ACKNOWLEDGEMENT

I appreciate the guidance and advice by Professors Suk Wang Yoon and Thomas B. Gabrielson.

Especially, I would like to say "Thank you very much" to David Gardner for answering so many of my questions and providing help with the computer programs.

And I also appreciate the help by my wife Heon-Ja Bang and my friend In-seop Park in conducting the experiment.

# I. INTRODUCTION

## A. OBJECTIVES

Identification of buried objects in the ocean bottom is an important problem in many fields such as oil exploration, geophysical research, and ocean engineering. A simpler problem is the identification of layers of infinite extent and unknown properties in the ocean sediments. The objectives of this thesis are:

1. to determine experimentally the depth of burial of a thin plate in a simulated sedimentary bottom;
2. to determine the sound speed and the thickness of the overlying sand layer; and,
3. to determine the sound speed and thickness of the thin plate.

It was the intent of this thesis to determine all of these properties by remote sensing with acoustic pulses in order to simulate an ocean measurement with a ship and near-surface sensors.

The first objective could have been accomplished by normal-incidence time-of-flight measurements; however, the second objective requires more information than that so a variable angle of incidence technique was used. This second objective was actually the principal goal since the third objective could not be achieved by using the technique described herein. The technique failed because the pulse could not be made short enough to distinguish the reflection

from the plate's lower surface. This is primarily the result of using very thin plates with respect to the acoustic wavelength. Perhaps the amplitude of the reflection from the top of the plate could be used to assist in identifying the plate material but the overlying sand layer makes this very difficult.

## B. APPROACH

The approach used is as follows:

1. Short pulses consisting of several cycles of a 150kHz sinusoidal wave were used as the source pulse.
2. A directional projector was used to minimize interference from surface and side-wall reflections.
3. The receiving hydrophone was mounted on a carriage so that the horizontal distance from source to receiver could be easily varied.
4. Each of the thin plates were buried in the sand bottom of a small water tank.
5. The plates were aluminum ranging in thickness from 0.1 to 1.8 cm and were buried at depths from 1.8 to 5.0 cm.
6. Two analytical methods were used for reducing the data. One method was based on the relationship between the square of the travel time (T) of the reflections and the square of the source-to-receiver horizontal range (X). The other method was based on maintaining a constant ray parameter (P) defined as the sine of the incident angle divided by the local sound speed.

## C. BACKGROUND

Reference 1 gives an excellent historical development of various seismological methods for determining properties of sediment layers. The following is a brief summary of that account.

Karcher and Haseman made the first successful seismic reflection measurements in 1921. Techniques for acoustic determination of sediment properties have advanced greatly since then and generally fall into one of three categories: normal incidence, wide-angle reflection, and refraction methods. Most of the development has been done by the petroleum exploration industry; however, the geophysical community has used these methods to study the earth's crust as early as the late 1930's. Dix, Krey and Dürbaum refined the sound speed measurements for sediment layers below the first layer by properly accounting for the shape of the arrival time as a function of range curves. By 1955, Dix had demonstrated the equivalence of T-X methc and $T^2$-$X^2$ method and, in 1968, Le Pichon refined the $T^2$-$X^2$ method until it became a standard analysis tool. A major enhancement was introduced by Bryan (see Ref. 2) in 1974 with the ray parameter method. Both the $T^2$-$X^2$ method and the ray parameter method were used in the data analysis for this thesis.

## II. THEORY

### A. T-X AND $T^2$-$X^2$ METHODS

A simple model of a layered sediment is shown in Fig. 2.1. The layers have thicknesses $H_1$, $H_2$ and $H_3$ and sound speeds $V_1$, $V_2$ and $V_3$. The $T^2$-$X^2$ method [Ref. 1] can be applied to this situation as described in this section.

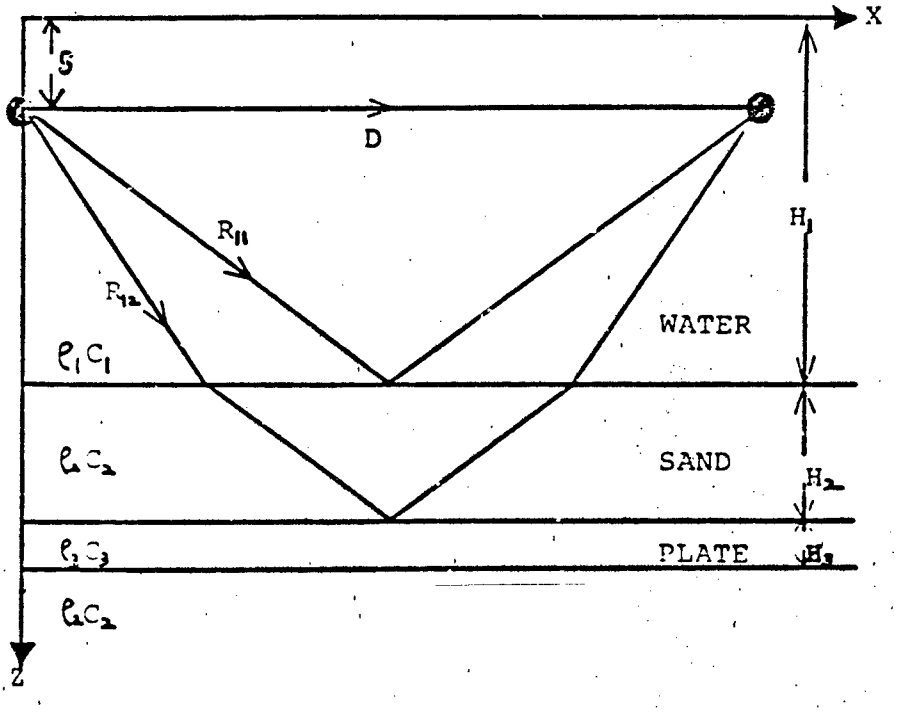


Figure 2.1. Geometry of Layers

For convenience, let the sound speed in the uppermost layer (the water layer) be less than that in the first

sediment layer. The length of the path that reflects from the top of the sediment layer is given by,

$$R_{11}^2 = X^2 + 4(H_1 - s)^2 \qquad (1)$$

To convert this to travel time squared, divide through by $V_1^2$:

$$T^2(X) = T^2(0) + (\frac{1}{V_1^2})X^2 \qquad (2)$$

where T(X) is the reflection travel time at horizontal range X and T(0) is the intercept of the travel time curve at X = 0. Since $T^2(0)$ is a constant, the reflection curve is a hyperbola. The corresponding curve for the direct path from the source to the receiver is a straight line and this hyperbola is asymptotic to that direct-path line.

When plotted in the $T^2$-$X^2$ plane, however, these lines are both straight. In this way, the slope of the reflection curves can be easily determined. As can be seen from the equation for the reflection path, the slope in the $T^2$-$X^2$ plane is $\frac{1}{V_1^2}$ which, in this thesis work, is calculated by linear regression of the $T^2$-$X^2$ data. This rather simple but accurate method is due to Green [Ref. 1] and is associated with the wide-angle seismic reflection technique.

The paths that pass through one or more sediment layers before reflection (see, for example, $R_{12}$ in Fig. 2.1) do not lead exactly to hyperbolas but the departure is not great

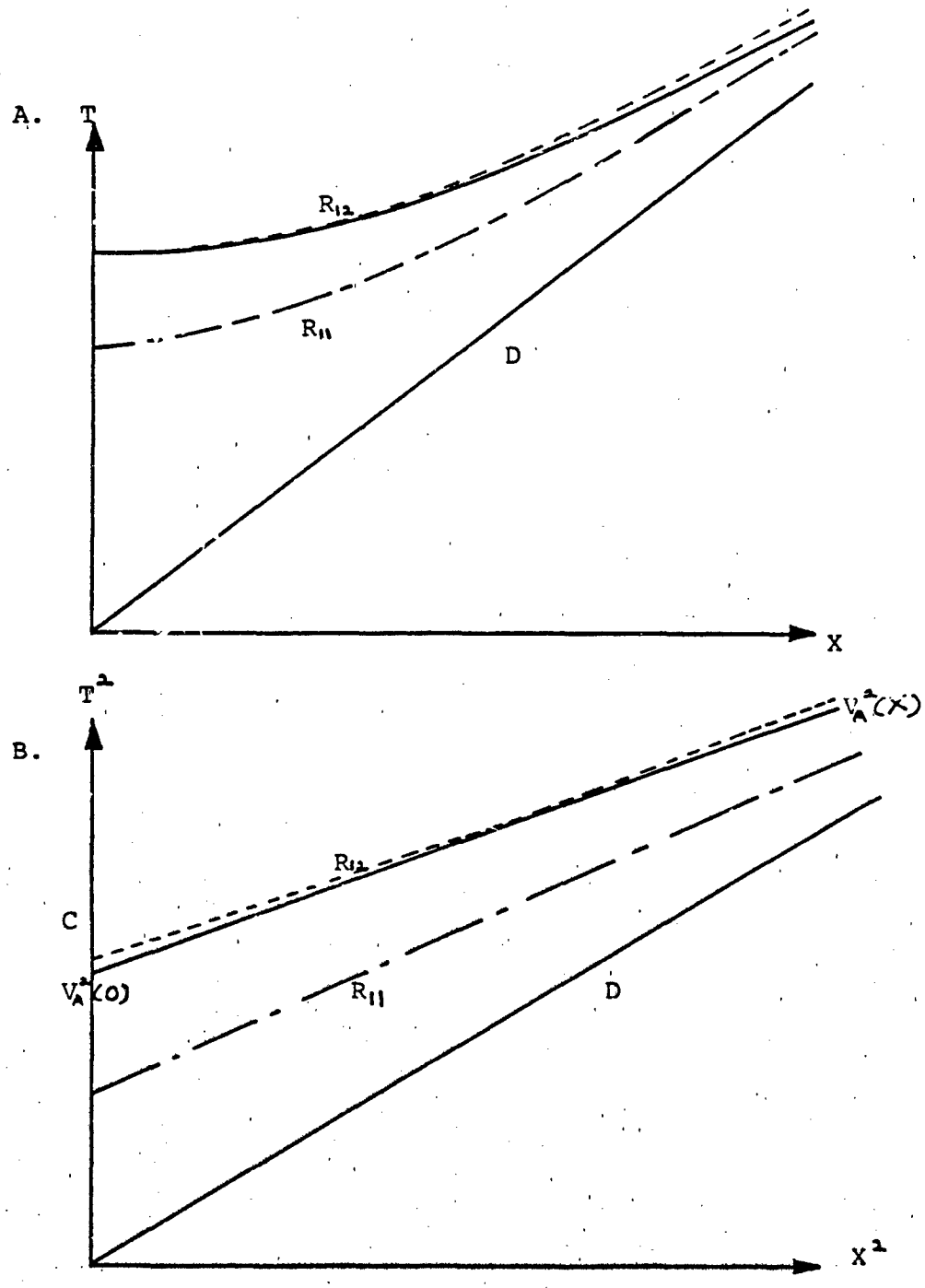


Figure 2.2. T-X and $T^2$-$X^2$ Curves

and only a small amount of error is introduced by fitting this data with straight lines in the $T^2$-$X^2$ plane.

If the layers were extremely thick or had great differences in sound speed, then the error might become appreciable. The reciprocal of the slope of the $R_{12}$ curve is equal to the average speed (squared) through both the water and the first sediment layer:

$$V = (H_1+H_2)/((H_1/V_1) + (H_2/V_2))$$

$$= (V_1T_1+V_2T_2)/(T_1+T_2) \qquad (3)$$

Representative T-X curves for this case are shown in Fig. 2.2.a. Curve D represents the direct path and $R_{11}$ represents the reflection curve for reflection from the top of the sediment. For $R_{12}$, the exact curve (solid line) is given as well as the hyperbola approximation (dotted curve) to that curve. The equivalent curves in $T^2$-$X^2$ space are shown in Fig. 2.2.b. Here the inverse slopes give the sound speed squared. The intercept T(0) gives the two-way vertical travel time through the layers.

The principal limitation of the $T^2$-$X^2$ method is shown in these figures. For any reflection other than the reflection from the top of the sediment, the curve is not exactly a straight line in $T^2$-$X^2$ coordinates but it falls slightly below the equivalent straight line as range increases.

B. THE RAY PARAMETER METHOD

In order to measure the properties of a layer without knowing the structure of the overlying layers, the ray parameter method can be used [Ref. 2]. Any ray path is specified by a fixed value of the ray parameter P defined by,

$$P = \sin \theta(z)/c(z) \tag{4}$$

where z is depth, c(z) is the sound speed profile and $\theta(z)$ is the angle that the ray makes with the vertical at depth z. Figure 2.3 shows the relationship between the incident angle and the ray parameter.

According to the ray parameter method, the increment of travel time along the ray path gives the corresponding increments in depth and range:

$$dz = c\,dT\cos\theta = (1 - P^2c^2)^{1/2} c\,dT \tag{5}$$

$$dX = c\,dT\cos\theta = P\,c^2dt = Pc(1 - P^2c^2)^{-1/2}dz \tag{6}$$

After integrating over depth from the surface to depth $z_1$, these expressions can be rewritten as follows,

$$T(P) = \int_0^{z_1} c^{-1}(1 - P^2c^2)^{-1/2}\,dz \tag{7}$$

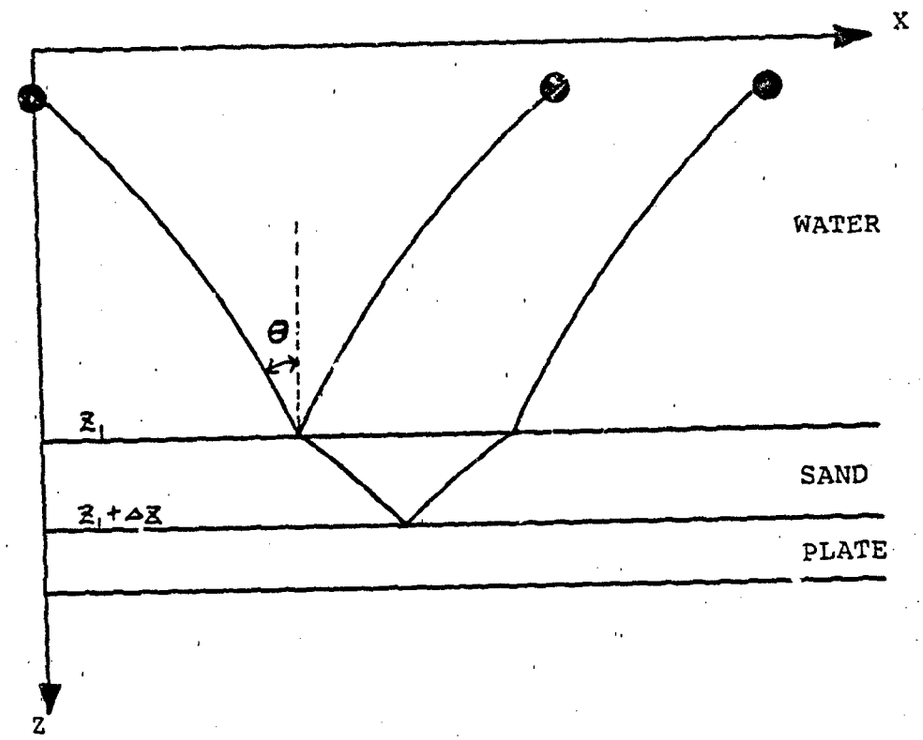


Figure 2.3. Geometry of Ray Parameter

$$X(P) = \int_0^{z_1} Pc(1 - P^2c^2)^{-1/2} dz \qquad (8)$$

These equations give the travel time T and the horizontal distance X along the ray path given by P in terms of integrals over depth. The equations must be solved for the sound speed variation c(z). This can be done for some special cases of layer structure.

...r a homogeneous layer (sound speed $c_1$) extending from $z_1$ to $z_1 + \Delta z$ (Fig. 2.3). For the ray of a particular ray parameter value, there are two (in this case) rays that

return from the bottom with that same parameter value although they arrive at the receiver at different ranges. Note that these rays are parallel through the water column. The travel time and horizontal distance for these two rays are, according to Eqs. (7) and (8),

$$\Delta T(P) = 2 \int_{z_1}^{z_1+\Delta z} c^{-1}(1 - P^2c^2)^{-1/2} dz \qquad (9)$$

$$\Delta X(P) = 2 \int_{z_1}^{z_1+\Delta z} Pc(1 - P^2c^2)^{-1/2} dz \qquad (10)$$

where the factor 2 accounts for the round trip of the ray. If the sound speed is constant at $c_1$ in the layer, these equations can be integrated to give,

$$\Delta T = 2c_1^{-1}(1 - P^2c^2)^{-1/2} \Delta z \qquad (11)$$

$$\Delta X = 2Pc_1(1 - P^2c_1^2)^{-1/2} \Delta z \qquad (12)$$

The expressions for sound speed and layer thickness are then,

$$c_1 = \left(\frac{1}{P} \frac{\Delta X}{\Delta T}\right)^{1/2} \qquad (13)$$

$$\Delta z = \frac{1}{2} c_1 \Delta T(1 - P^2c_1^2)^{1/2} \qquad (14)$$

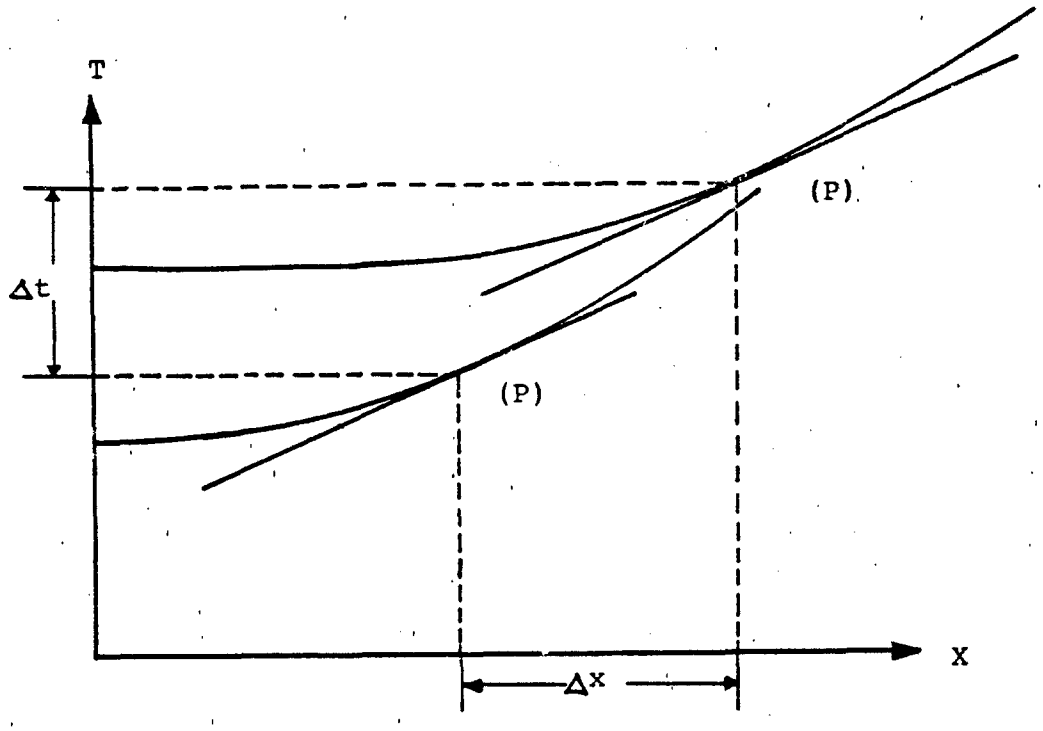


Figure 2.4. T-X Curve and the Ray Parameter

The important feature of the ray parameter method is that the structure above the layer has dropped out because of the choice of ray path.

In order to apply this technique in practice, an initial value of ray parameter was chosen based on a geometry that gives good clean reflection signals. After the T-X curves are drawn, this value of ray parameter, which gives the slope of the T-X curves at the points of interest, was used to identify the two parallel return rays. The principal difficulty of this method is that the T-X curves are not straight lines and, therefore, curves must be fit to the

experimental data. This introduces some uncertainty into the process but, fortunately, the values for layer thickness is not very sensitive to the type of fit that is done.

## III. EXPERIMENTAL PROCEDURES

### A. ARRANGEMENT OF THE EXPERIMENT

The measurements were made in a tank which was 300 cm long, 115 cm wide and 90 cm deep. The tank was filled with carefully de-aerated (fresh) water and had a 55 cm deep sand bottom (also de-aerated).

At first, an ITC 501 projector was used but the beam pattern was fairly broad leading to excessive reflections from the surface and the side-walls and, more importantly, this projector was large enough so that it would ring for a significant length of time compared to the desired pulse length. As a result, the output pulse was too long regardless of the length of the pulse used as input.

These problems led to the selection of a USRF F-41 projector, which is a directional laboratory standard transducer used in acoustic reciprocity calibrations over the frequency range from 15 to 150 kHz. This projector consists of lead zirconate-titanate elements cemented to a high-density kennametal disks. The resulting array of elements is about 3.8 cm wide and 5 cm high.

The receiving hydrophone used was an omnidirectional LC-10 hydrophone mounted on a carriage that was free to roll along tracks installed on the long sides of the tank. In this way the horizontal distance (X) could be easily varied.

A block diagram of the electronics used is shown in Fig. 3.1. The digital oscilloscope was used to measure the time differences between various pulses. In order to reject unwanted noise, a filter was used to pass only 100 kHz to 200 kHz.

The choice of pulse length was governed by the criteria that it be (1) long enough to reach steady-state conditions in the projector and (2) short enough to resolve the individual reflections from the layers. The best compromise turned out to be four cycles of a 150 kHz sine wave, but, unfortunately, this was not short enough to completely define the thin plate. At 150 kHz, one cycle is 6.7 μS so the four-cycle pulse was about 27 μS long. A typical received signal using the four-cycle pulse is shown in Fig. 3.2 while Fig. 3.3 shows the same situation with an eight-cycle pulse. The four-cycle pulse gives much better definition of individual arrivals.

Before the actual measurements were made, several tests were performed in order to insure that side-wall and surface reflections would not interfere with the measurements. The depths of the projector and hydrophone were determined by trial and error not only to minimize interfering reflections but also to optimize the separation between the desired arrivals. In addition, this set a practical limit on the horizontal range.

An attempt was made to move the axis of the source-to-receiver line toward the tank wall so that two parallel

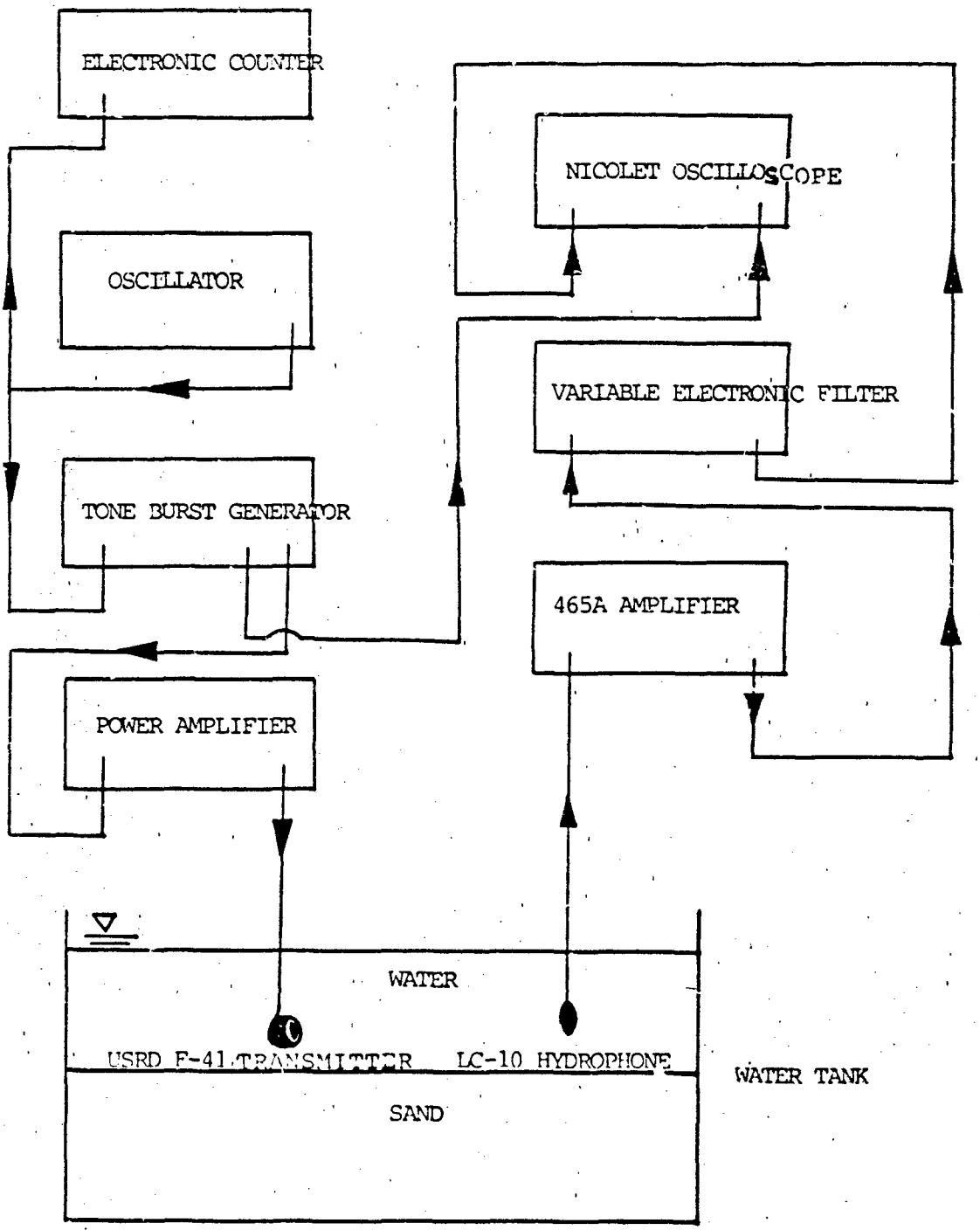


Figure 3.1. Block Diagram

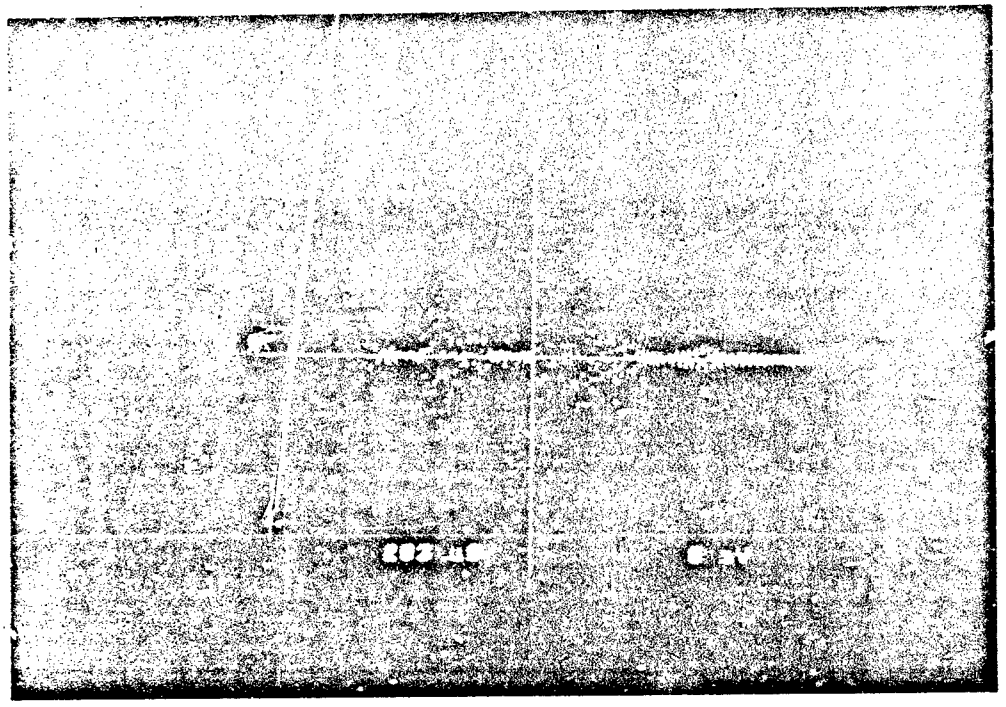

Figure 3.2. 4 Cycle Pulse Signal

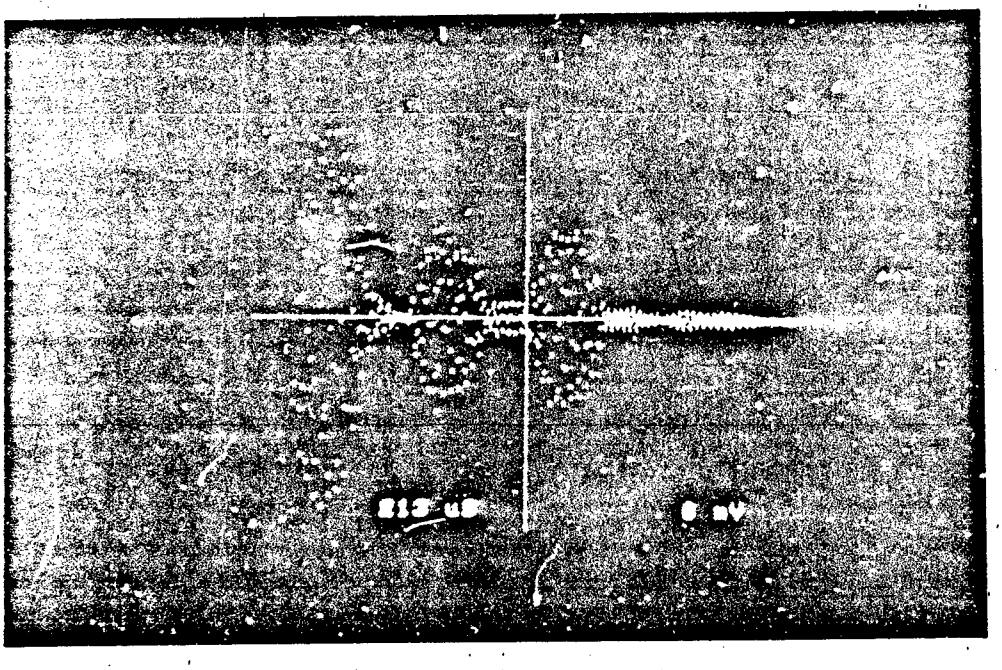

Figure 3.3. 8 Cycle Pulse Signal

measurements could be made without disturbing the sand to bury each plate. This introduced unacceptable side-wall

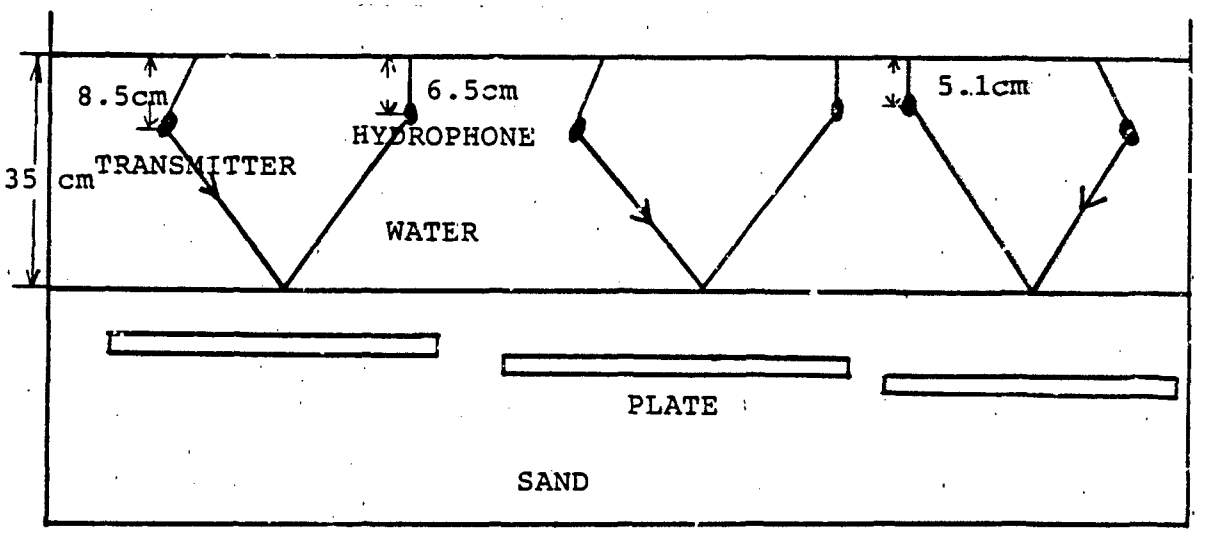


Figure 3.4. Location of Projector, Hydrophone and Plates

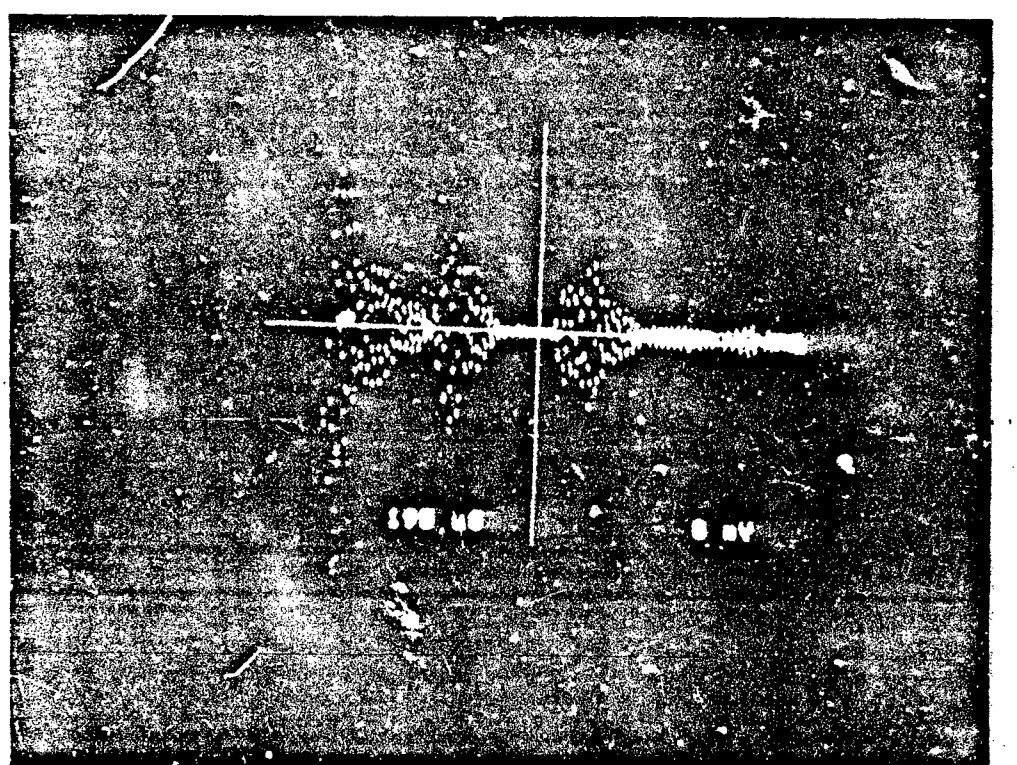

Figure 3.5. Projector Is Not on the Center Line

reflections so, instead, three plates were buried in line along the long axis of the tank with the projector and receiver positioned as shown in Fig. 3.4.

Here, the plates were buried at different depths and the projector and hydrophone were positioned as shown. (Notice that in the third set-up on the right the source and receiver are reversed to avoid reflections from the end-wall.)

Figure 3.5 shows the side-wall reflections that are introduced when the source-to-receiver axis is displaced only 15 cm toward one side of the tank. This result should be comparable to Fig. 3.2 but only a position along the centerline of the tank turned out to be acceptable.

## B. EXPERIMENTAL PROCEDURE

Once the experiment was set up, the first step was to identify the individual arrivals from a particular buried plate. By considering the projector depth S, the hydrophone depth h, the water depth H, the major incident angle, and the slant distance R, the time of arrival of the various reflections was determined by simple image theory [Ref. 3, pp. 427-429]. A representative diagram of the various arrivals is shown in Fig. 3.6 for constant sound speed in the water layer.

Since a directional projector was used and was aimed downward toward the sediment, the surface-reflected path 7 could be neglected. For most of the measurements, paths 1, 3 and 4 were used.

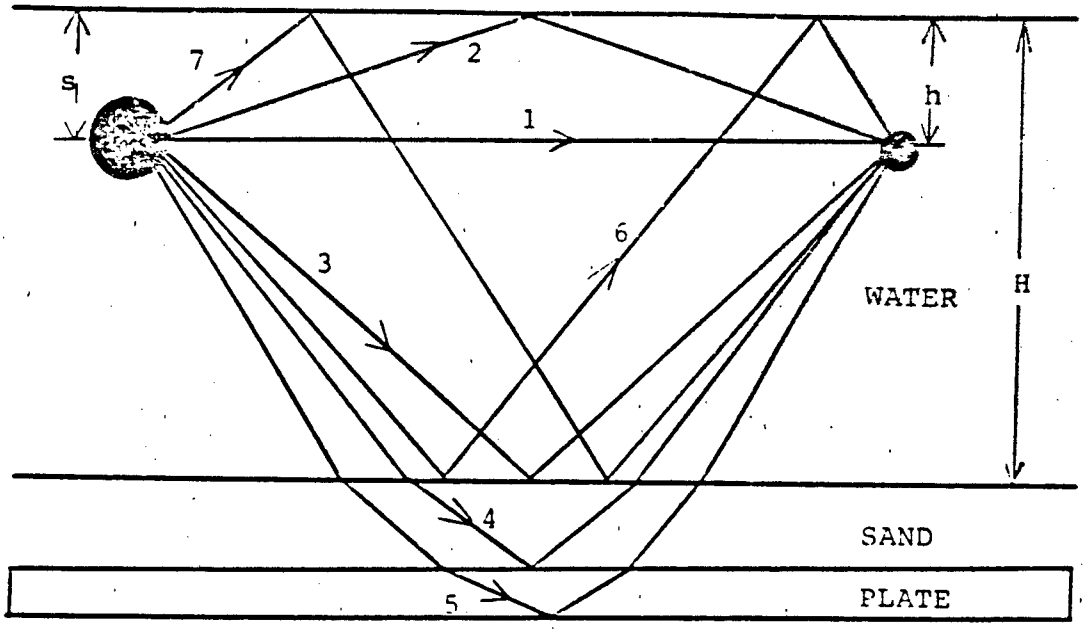


Figure 3.6. Waves in the Isospeed Shallow Water Channel

Basically, three methods were used to initially identify the arrivals on the digital oscilloscope. First, the arrival times predicted by the method of images were compared to the measured arrival times. The amplitude of the arrivals also helps in the identification process since the pressure amplitude is reduced by the reflection coefficient at each of the interfaces of the layers. Finally, a path that reflects from the surface can be readily identified by disturbing the water's surface with a ruler. Any surface-reflected arrivals change greatly on the oscilloscope display and can easily be separated from those arrivals that only reflect from the bottom.

A typical display on the oscilloscope is shown in Fig. 3.7. Here, the projector is inclined so that the beam has an incident angle of 55 degrees and the water depth is 35 cm. The arrivals shown are:

1. direct wave,
2. surface-reflected wave,
3. bottom-reflected wave,
4. wave reflected from the top of the plate,
5. wave reflected from the bottom of the plate after passing through the plate,
6. bottom-surface-reflected wave.

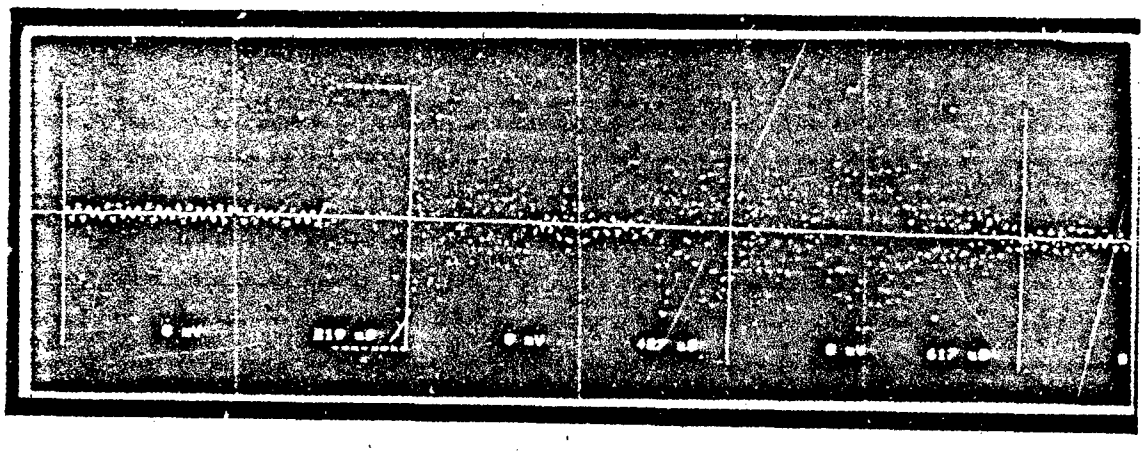


Figure 3.7. Different Kinds of Waves on Oscilloscope

Once the arrivals are identified for one source-to-receiver range, the signals can be followed by eye if the receiver carriage is moved smoothly.

Next, the range X is varied by moving the carriage and the arrival times T of the individual reflections are recorded. These measurements form the basis of the T-X and $T^2$-$X^2$ methods. When these measurements are plotted as arrival time T as a function of range X, the direct arrivals appear as straight lines and the reflected arrivals (either from the top of the sand layer or from any of the layers below) appear as parabolas. (They are actually closer to hyperbolas but, over the limited range available in this experiment, parabolas were used as an approximation.)

The T and X measurements were also plotted as $T^2$ as a function of $X^2$. On these coordinates, any of the lines are straight (or nearly so). From the slope of these lines, the sound speed either in the water or in the layers could be calculated. A linear regression method was used to compute the slope for the individual arrivals.

Next, the ray parameter P was calculated. This value is fixed for a given measurement. The incident angle was determined from the source-receiver geometry and the T-X data were fit with parabolas. Then P could be calculated directly from the parabola equation: $T = aX^2 + bX + c$, $dT/dX = P = 2aX + b$.

Once the parabolas have been determined, the layer depth found from the T-X measurements. For example, the

arrival from the wave that passed through the upper sand layer would be described by a parabcla of the form $T_1 = a_1X_1^2 + b_1X_1 + c_1$ and the reflection from the top of the sand layer would be given by $T_2 = a_2X_2^2 + b_2X_2 + c_2$. The ray parameter P must be the same for each arrival; therefore, for the wave passing through the sand layer, $P = 2a_1X_1 + b_1$ or $X_1 = (P-b_1)/2a_1$, and, for the wave reflected from the top of the sand layer, $P = 2a_2X_2 + b_2$ or $X_2 = (P-b_2)/2a_2$. Since $\Delta X = X_1-X_2$,

$$\Delta T = [\{a_1(\frac{P-b_1}{2a_1})^2 + b_1(\frac{P-b_1}{2a_1}) + c_1\} - \{a_2(\frac{P-b_2}{2a_2})^2 + b_2(\frac{P-b_2}{2a_2}) + c_2\}]$$

These two values (T and X) are necessary to calculate the depth and the sound speed (to compare with the $T^2$-$X^2$ determination of sound speed) of the layer. The values of layer depth $\Delta z$ and sound speed $c_1$ are given by,

$$\Delta z = \frac{1}{2} c_1 \Delta T (1 - P^2c_1^2)^{1/2}$$

The first value of $c_1$ is from the $T^2$-$X^2$ method and $\Delta T$ is from the parabolic fit of the T-X data. The new value of $c_1$ can be compared to the old value as a check on the two methods.

C. SUMMARY OF EXPERIMENTAL PROCEDURE

1. Bury the thin homogeneous plates at various depths;
2. Identify the arrivals on the oscilloscope;

3. Measure the horizontal distance X and the arrival time T of the various arrivals;

4. Make the T-X and $T^2$-$X^2$ plots;

5. Find the sound speed $c_1$ in the layer by using the $T^2$-$X^2$ method;

6. Determine the incident angle from the source-receiver geometry;

7. Calculate the ray parameter P (fixed for each experiment);

8. Fit the T-X data with parabolas;

9. Calculate $\Delta X$ and $\Delta T$ by the ray parameter method;

10. Calculate the layer depth $\Delta z$;

11. Calculate $c_1$ and compare to the value determined previously.

## IV. ANALYSIS AND RESULTS OF EXPERIMENTS

### A. MEASUREMENT AND ANALYSIS

A measurement of the sound speed in the water was required for each of the reflection analyses so this was measured using the $T^2$-$X^2$ method. The slope of the straight line fit to the data points gave a sound speed of 1447 m/s and the correlation coefficient associated with the linear regression was almost 100%. For this measurement, the projector beam was aimed horizontally and the hydrophone was positioned at the same depth as the projector.

In each of the subsequent experiments, the projector and hydrophone depths were chosen to optimize the separation and clarity of the reflection signals. In every case, the source signal was four cycles of a 150 kHz sine wave.

#### 1. Measurement 1

For this experiment an aluminum plate (thickness of 1.7 cm) was buried 3.5 ± 0.05 cm below the sand's surface and the projector depth was 8.5 cm while the hydrophone depth was 6.5 cm.

TABLE I

Speed of Sound (Measurement 1)

| WAVE | SPEED OF SOUND (m/s) | CORRELATION (%) | ERROR (%) |
|---|---|---|---|
| SAND | 1661 | 98.3 | |
| BOTTOM | 1415 | 99.4 | 2.2 |
| DIRECT | 1463 | 99.8 | 1.1 |

Table I gives the speed of sound calculated from the various arrivals along with the correlation coefficients of the linear regressions. The speed of sound in the water should be compared to the value of 1447 m/s discussed above. The T-X and $T^2$-$X^2$ data are shown in Fig. 4.1.

As discussed in the previous chapter, the T-X data were fit with a parabola for simplicity. The data for the wave that reflected from the top of the aluminum plate was fit with

$$T = 0.0926\ X^2 - 2.89\ X + 459$$

and the data for the wave that reflected directly from the top of the sand was fit with

$$T = 0.113\ X^2 - 3.03\ X + 410$$

The geometry selected for the ray parameter determination gave an incident angle of 29 degrees which corresponds to a ray parameter P equal to $3.32 \times 10^{-6}$ s/m. This value of slope locates a point on each of the two parabolas. The difference in X values gives a $\Delta X$ of 5.47 cm. The parabolic form for the reflection from the top of the plate gives the time difference $\Delta T$ of 51.4 μS.

Next, the layer thickness $\Delta z$ was calculated from Equation (14). In this case, $\Delta z$ was determined to be 3.56 cm. This differs by only 0.3% from the measured value for the

Figure 4.1. T-X and $T^2$-$X^2$ Plots (Measurement 1)

overlying sand layer. (The burial depth of the plate gives the thickness of the top sand layer.) The value for the layer's sound speed was also calculated from the ray parameter method but its value was not significantly different from that calculated by the $T^2$-$X^2$ method.

2. Measurement 2

For the second measurement, the hydrophone depth was 6.4 cm, the projector depth was 8.5 cm and the aluminum plate (1.7 cm thick) was buried at a depth of 2.9 ± 0.1 cm in the sand. The calculated sound speeds are given in Table II and the T-X and $T^2$-$X^2$ data are shown in Fig. 4.2.

TABLE II

Speed of Sound (Measurement 2)

| WAVE | SPEED OF SOUND (m/s) | CORRELATION (%) | ERROR (%) |
|---|---|---|---|
| SAND | 1647 | 94.3 | |
| BOTTOM | 1419 | 99.6 | 1.96 |
| DIRECT | 1437 | 99.1 | 0.69 |

Figures 4.3 and 4.4 show representative displays from the oscilloscope at two of the ranges at which measurements were taken.

The direct wave (A), the surface-reflected wave (B), the wave that reflects from the top of the sand (C), the wave that reflects from the top of the buried plate (D), and

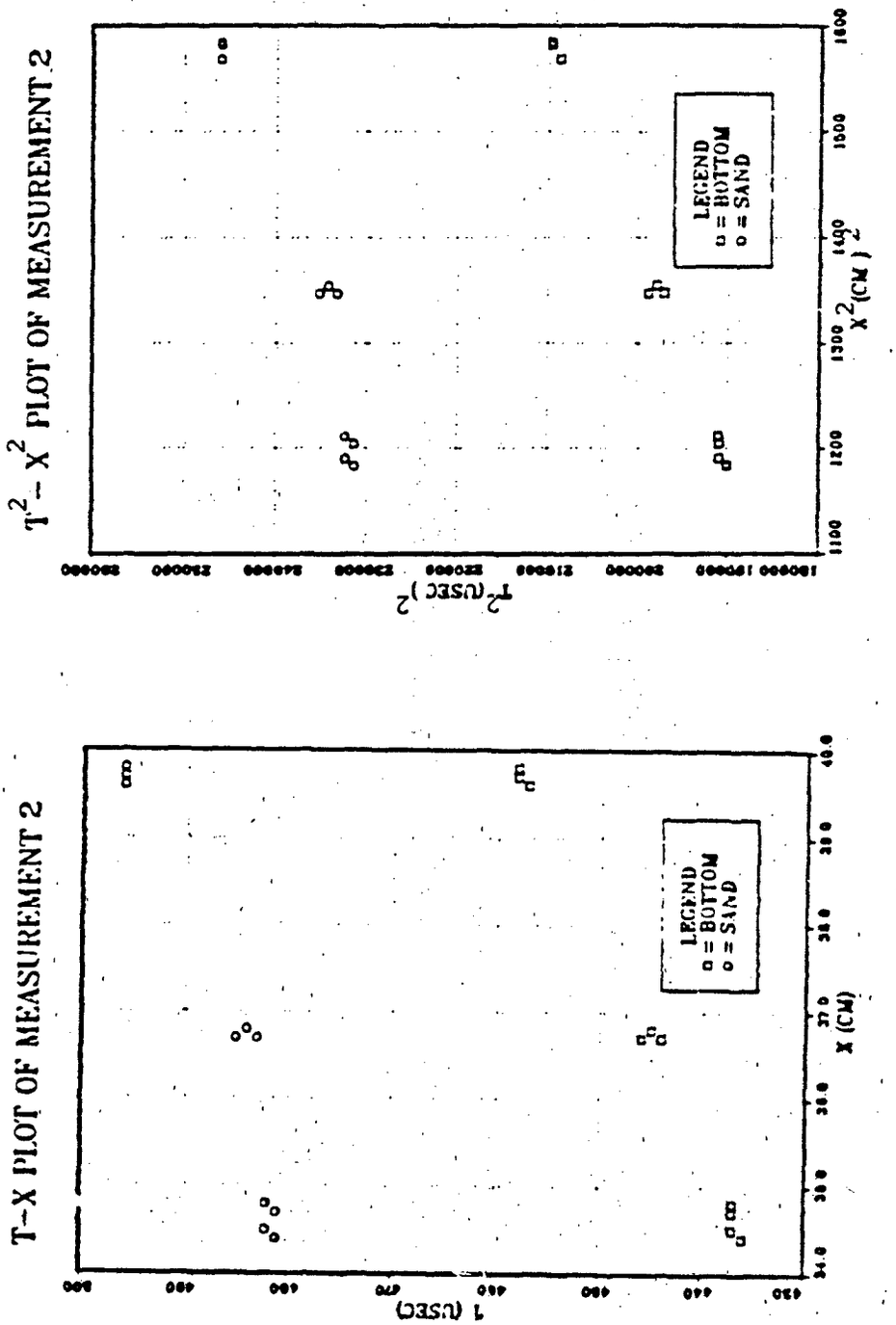


Figure 4.2. T-X and $T^2$-$X^2$ Plots (Measurement 2)

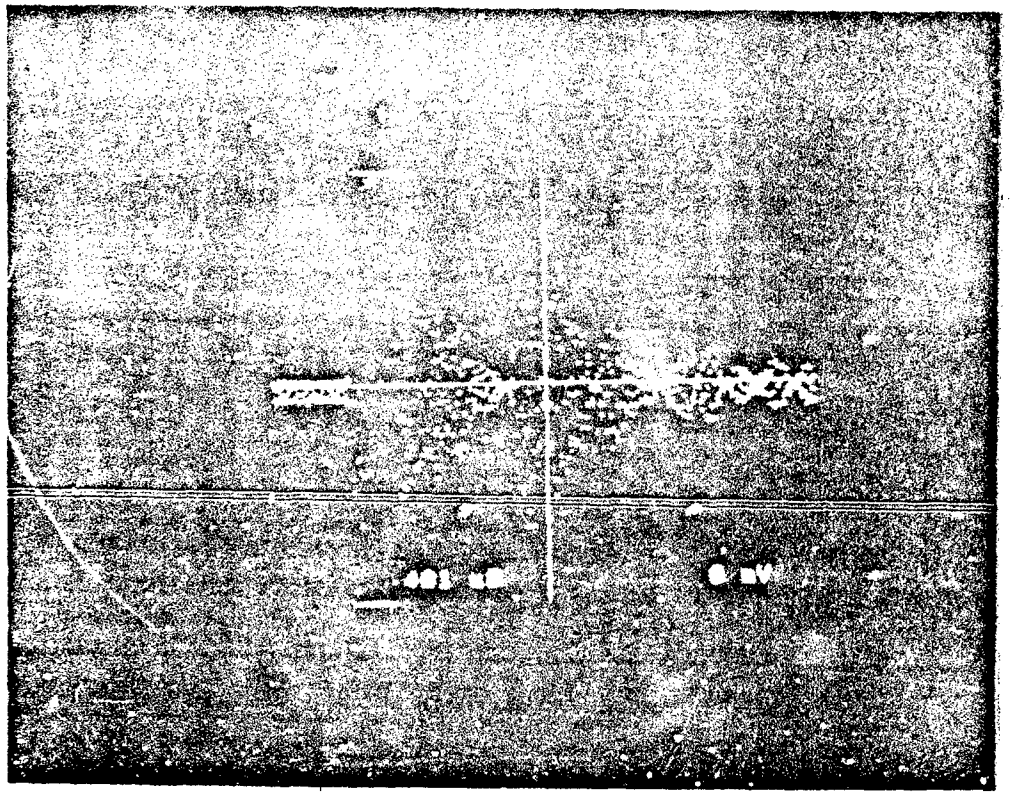

Figure 4.3. Measurement 2 at X = 34.5 cm.

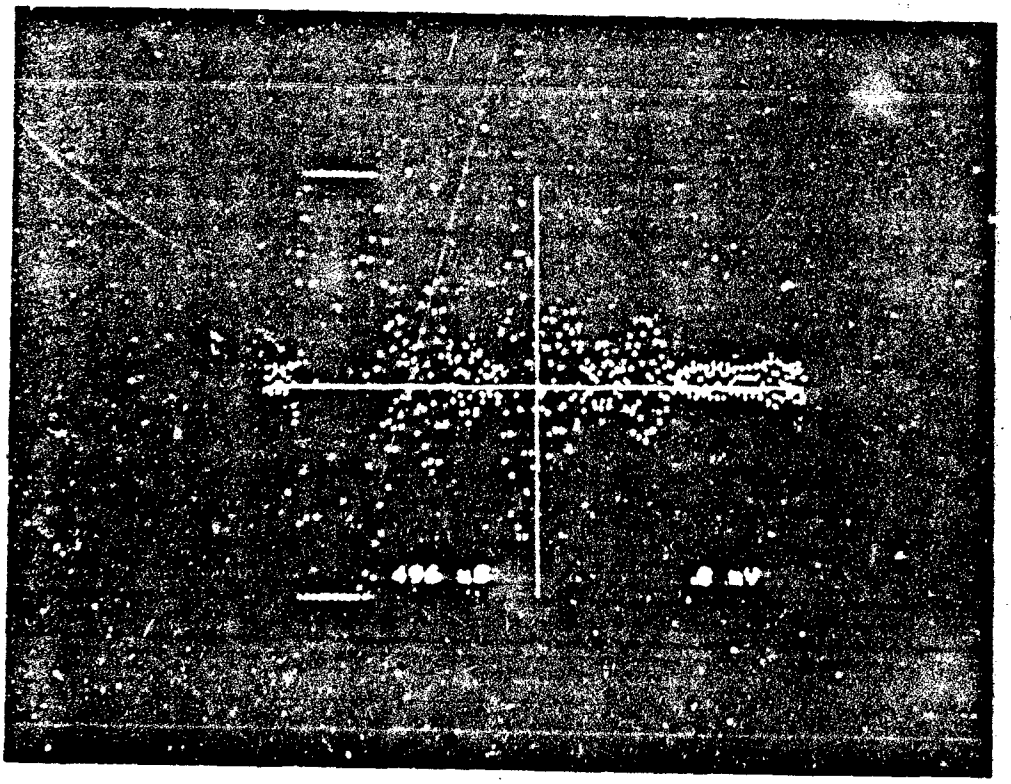

Figure 4.4. Measurement 2 at X = 39.6 cm.

the wave that reflects from the top of the sand and again from the water surface (E) are shown in these figures. The vertical line marks the beginning of the wave that is reflected from the top of the plate and the number gives the arrival time.

In this case, the curve for the arrival reflected from the top of the plate is,

$$T = 0.473\ X^2 - 32.0\ X + 1020$$

and the curve for the arrival reflected from the top of the sand is,

$$T = 0.136\ X^2 - 5.72\ X + 471$$

Here, the incident angle was 28.3 degrees so P was $3.30 \times 10^{-6}$ s/m. The ray parameter calculations gave 3.87 cm for $\Delta X$ and 54 μS for dT so the layer depth $\Delta z$ was 3.73 cm. The actual sand layer thickness was 3.4 cm so the error was slightly less than 10%. The value for sound speed in the water by the ray parameter method was 1474 m/s which is about 10% high.

3. Measurement 3

In this measurement, an aluminum plate 0.1 cm thick was buried to a depth of 2.3 ± 0.1 cm. The projector depth was 8.5 cm and the hydrophone depth was 5.1 cm. The resulting speed of sound measurements (determined by the $T^2$-$X^2$ method) are summarized in Table III and the T-X data and the

$T^2$-$X^2$ data are shown in Fig. 4.5. Figures 4.6 and 4.7 show representative displays from the oscilloscope at two of the ranges at which measurements were taken.

TABLE III

Speed of Sound (Measurement 3)

| WAVE | SPEED OF SOUND (m/s) | CORRELATION (%) | ERROR (%) |
|---|---|---|---|
| SAND | 1649 | 95.2 | |
| BOTTOM | 1471 | 99.9 | 1.7 |
| DIRECT | 1510 | 99.8 | 4.3 |

The parabola for the arrivals reflecting from the top of the plate was determined to be

$$T = 0.290\ X^2 - 13.3\ X + 580$$

and the parabola for the arrivals directly reflected from the top of the sand is

$$T = 0.0484\ X^2 + 0.528\ X + 357$$

For the optimum geoemtry, the incident angle was 27 degrees so that the ray parameter P was $3.00 \times 10^{-6}$.

The ray parameter analysis gave 2.53 cm for $\Delta X$ and 33.38 μs for $\Delta T$; therefore, the sand layer depth was computed to be 2.42 cm: less than one percent from the actual value.

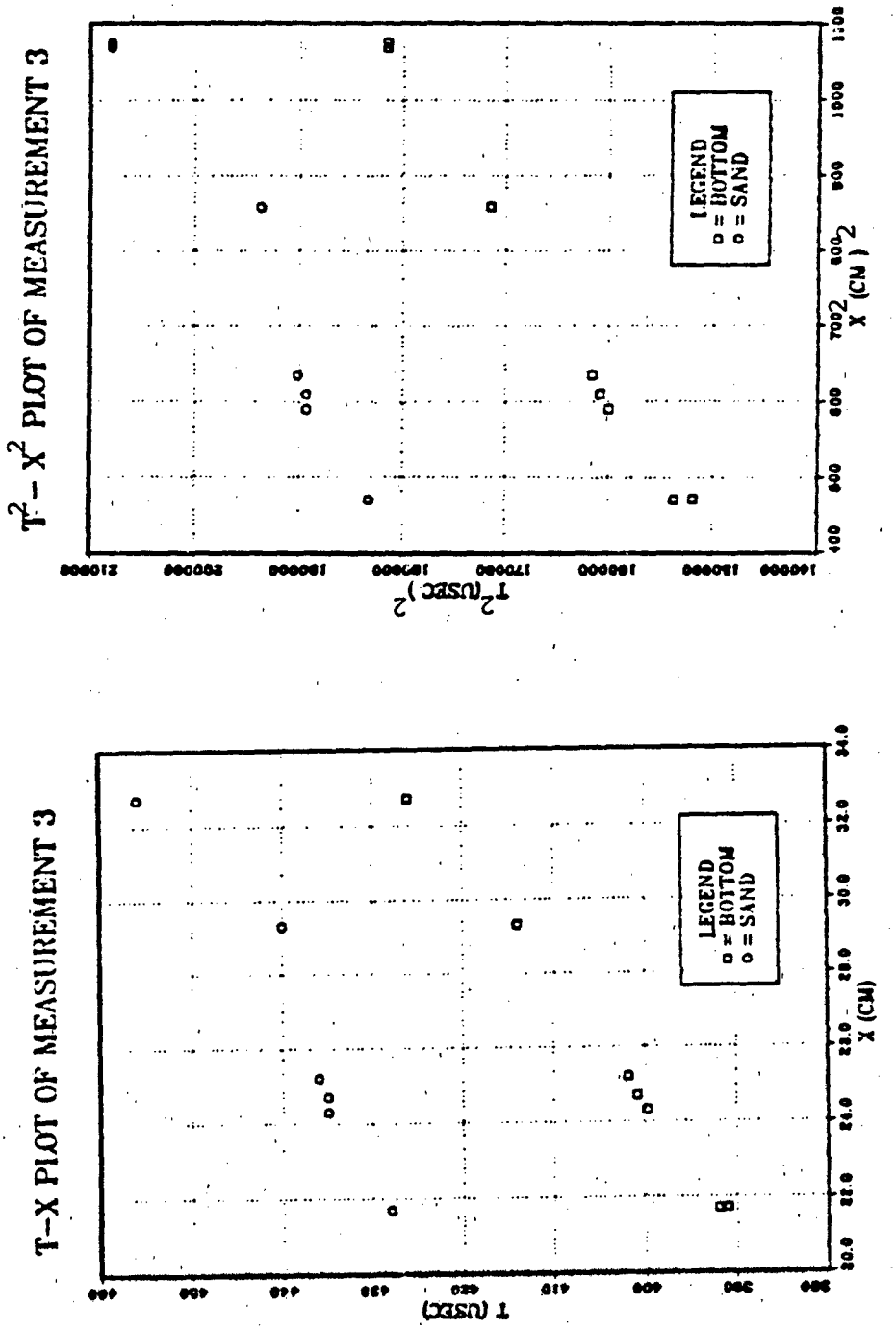


Figure 4.5. T-X and $T^2$-$X^2$ Plots (Measurement 3)

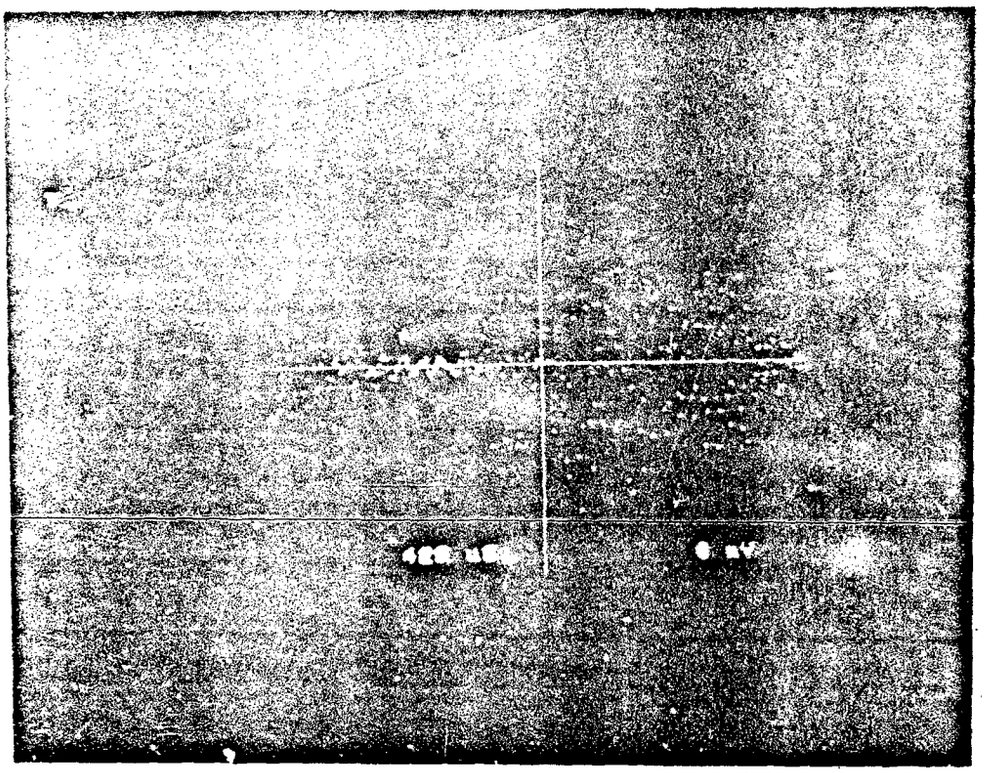

Figure 4.6. Measurement 3 at X = 21.7 cm.

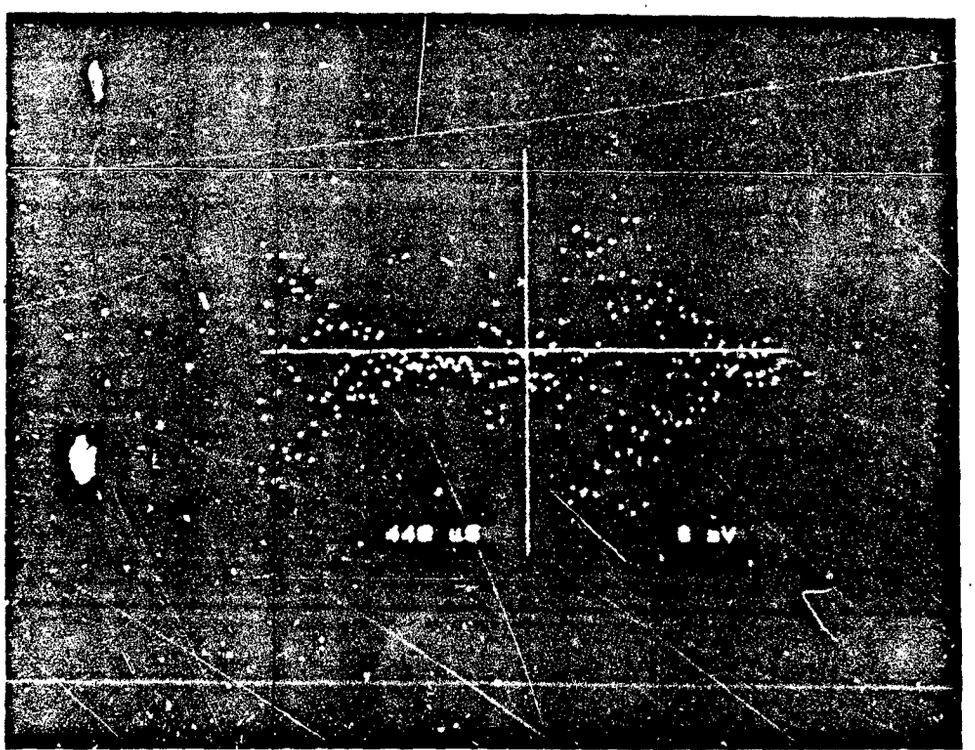

Figure 4.7. Measurement 3 at X = 29.3 cm.

The calculated value for the sound speed in the sand layer was 1578 m/s and this differs by only 3 percent from the value obtained by the $T^2-X^2$ method.

4. Measurement 4

For this measurement, an aluminum plate 0.3 cm thick was buried to a depth of 1.8 ± 0.1 cm. The projector depth was 8.5 cm and the hydrophone depth was 3.5 cm. The speed of sound measurements is summarized in Table IV and the T-X data and the $T^2-X^2$ data are shown in Fig. 4.8. Representative displays from the oscilloscope at two ranges are shown in Figures 4.9 and 4.10.

TABLE IV

Speed of Sound (Measurement 4)

| WAVE | SPEED OF SOUND (m/s) | CORRELATION (%) | ERROR (%) |
|---|---|---|---|
| SAND | 1582 | 99.7 | |
| BOTTOM | 1458 | 99.7 | 0.7 |
| DIRECT | 1461 | 99.9 | 1.0 |

The parabolic form for the reflections from the top of the plate is

$$T = 0.0259\ X^2 + 0.361\ X + 429$$

and the form for the reflections from the top of the sand is

$$T = 0.0328\ X^2 + 1.17\ X + 380$$

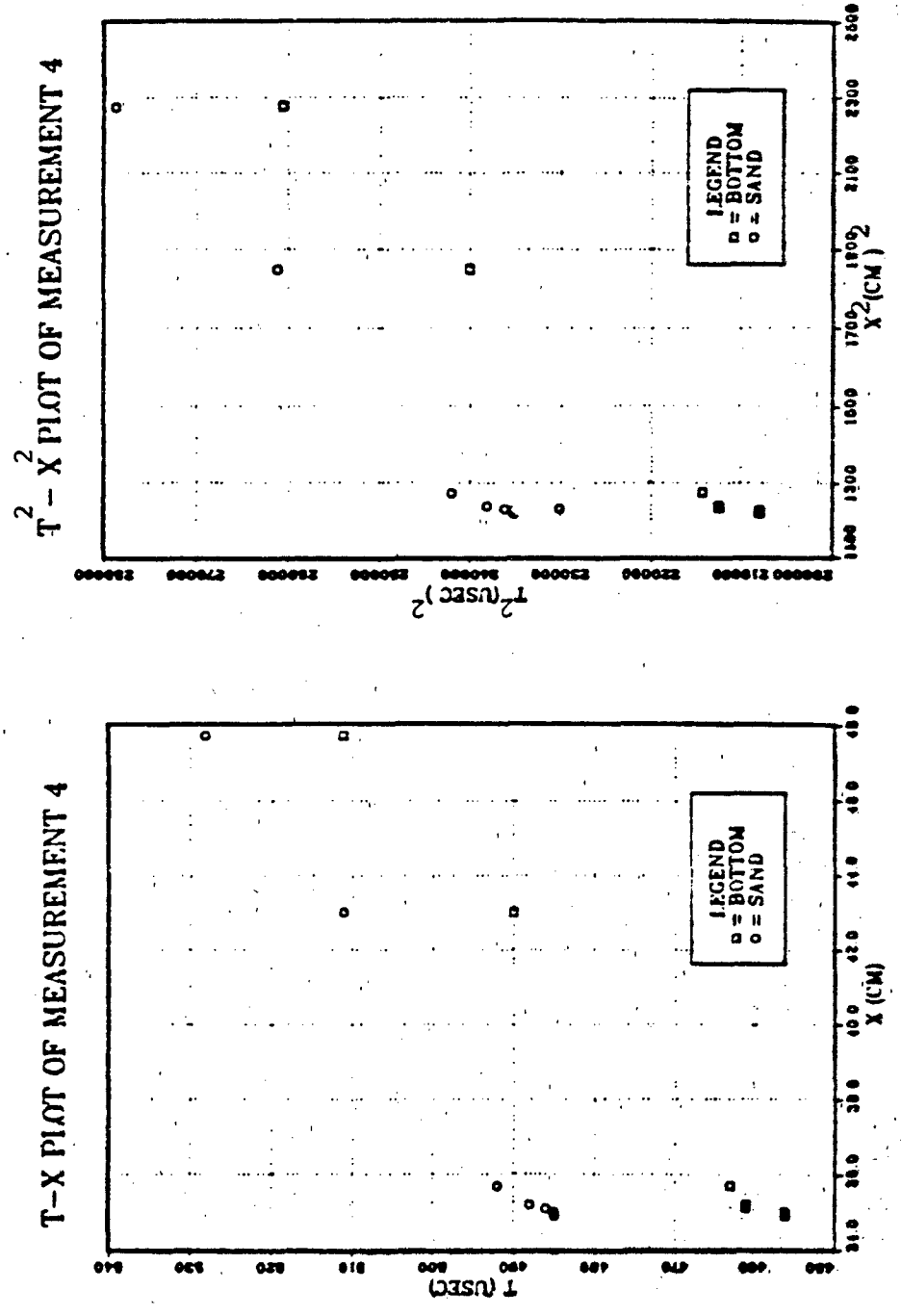


Figure 4.8. T-X and $T^2$-$X^2$ Plots (Measurement 4)

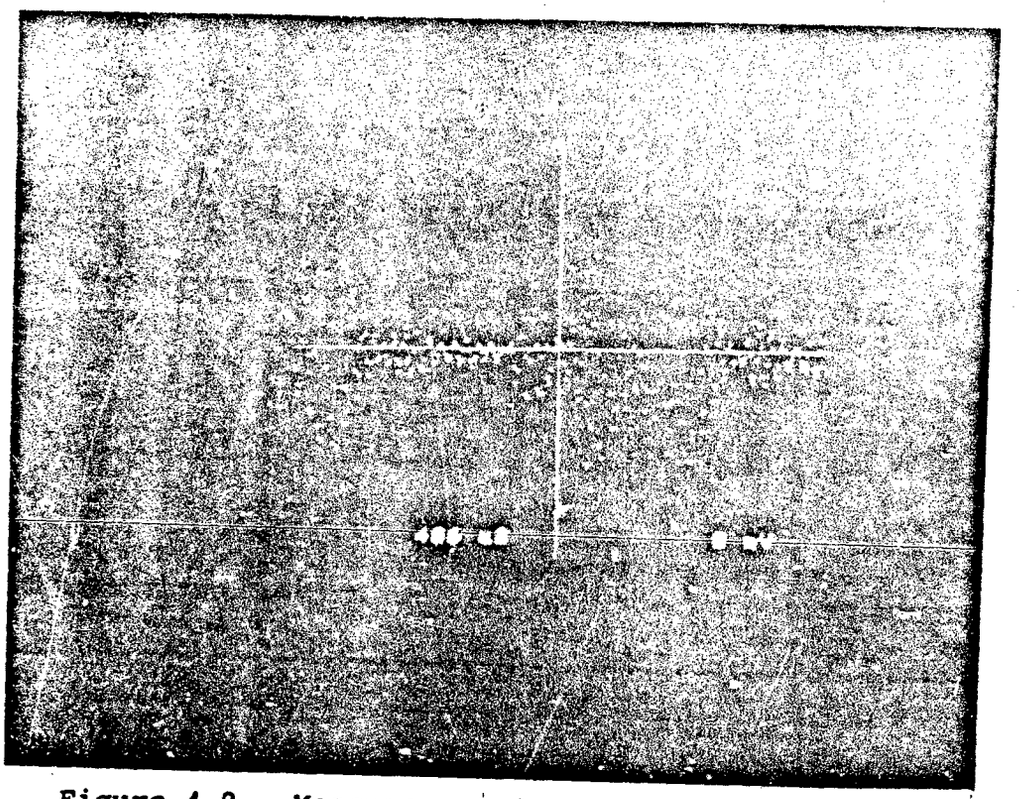

Figure 4.9. Measurement 4 at X = 35.1 cm.

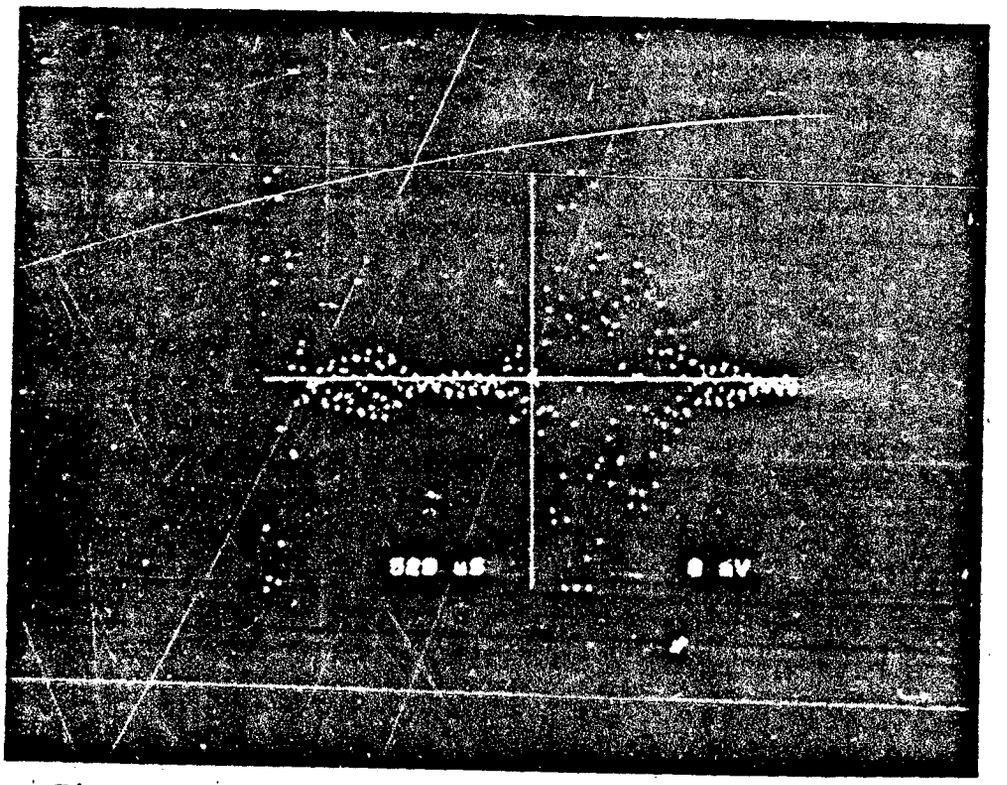

Figure 4.10. Measurement 4 at X = 47.7 cm.

For the optimum geometry, the incident angle was 50 degrees so that the ray parameter P was $5.3 \times 10^{-6}$.

The ray parameter analysis gave 5.80 cm for $\Delta X$ and 40.4 μs for $\Delta T$; therefore, the sand layer depth was computed to be 1.74 cm. The calculated value for the sound speed in the sand layer was 1647 m/s. In both cases, the results compare very well with the measured value for layer depth and the $T^2-X^2$ value for sound speed.

5. Measurement 5

For this measurement, the projector depth was 8.5 cm and the hydrophone depth was 3.5 cm. The aluminum plate (0.1 cm thick) was buried at a depth of 5.0 ± 0.1 cm. The speed of sound measurements are summarized in Table V and the T-X data and the $T^2-X^2$ data are shown in Fig. 4.11. Samples of the received arrivals at two ranges are shown in Figures 4.12 and 4.13.

TABLE V

Speed of Sound (Measurement 5)

| WAVE | SPEED OF SOUND (m/s) | CORRELATION (%) | ERROR (%) |
|---|---|---|---|
| SAND | 1577 | 99.9 | |
| BOTTOM | 1468 | 100 | 1.4 |
| DIRECT | 1488 | 100 | 2.8 |

The parabolic form for the reflections from the top of the plate is

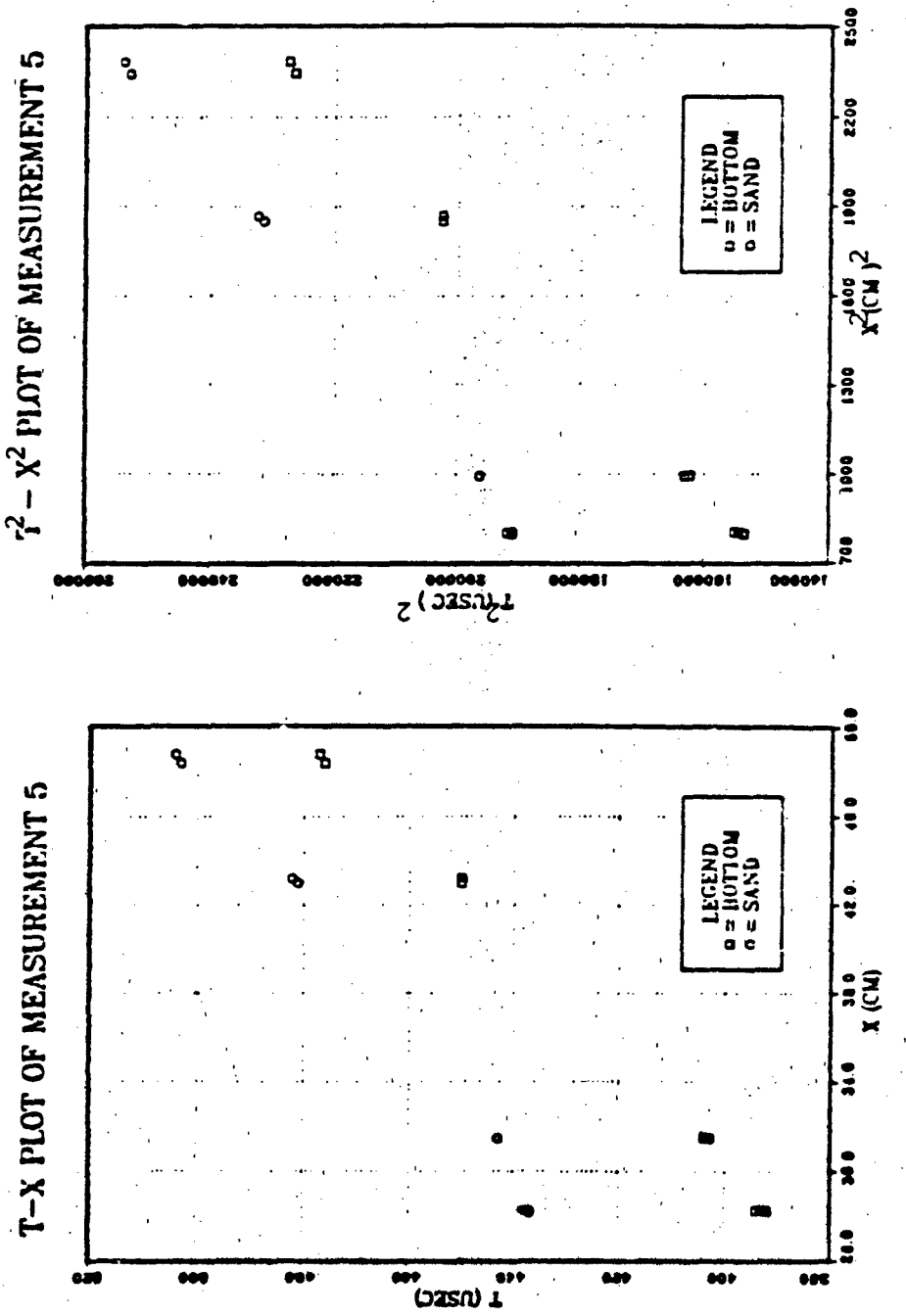


Figure 4.11. T-X and $T^2$-$X^2$ Plots (Measurement 5)

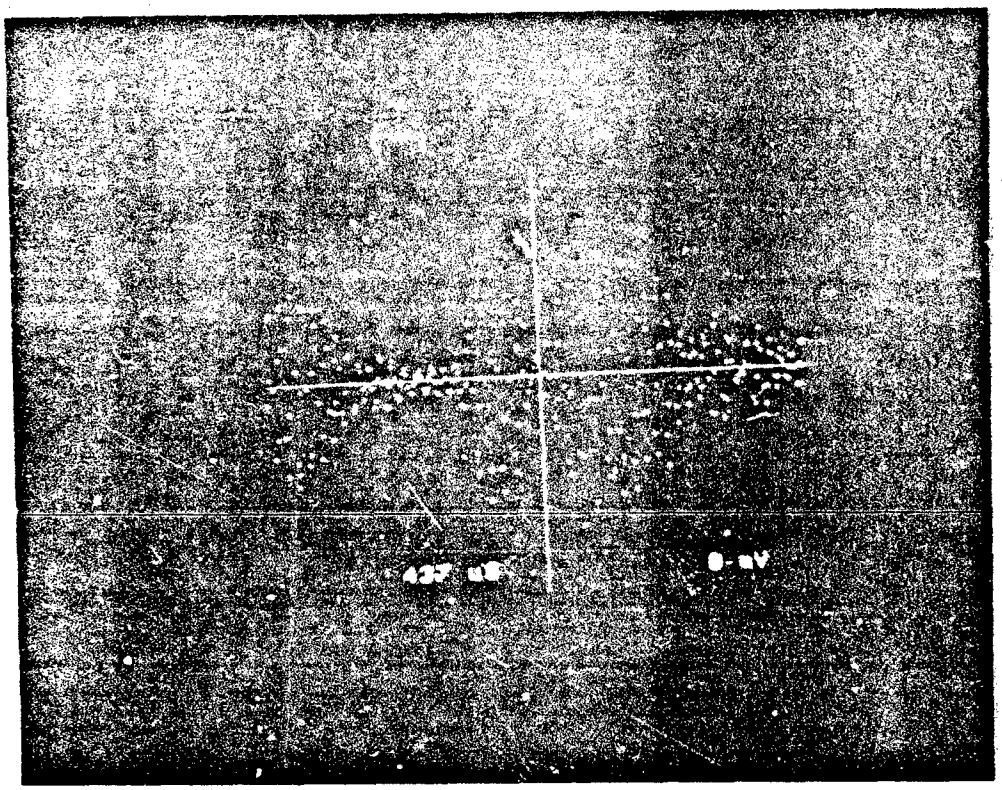

Figure 4.12. Measurement 5 at X = 28.2 cm.

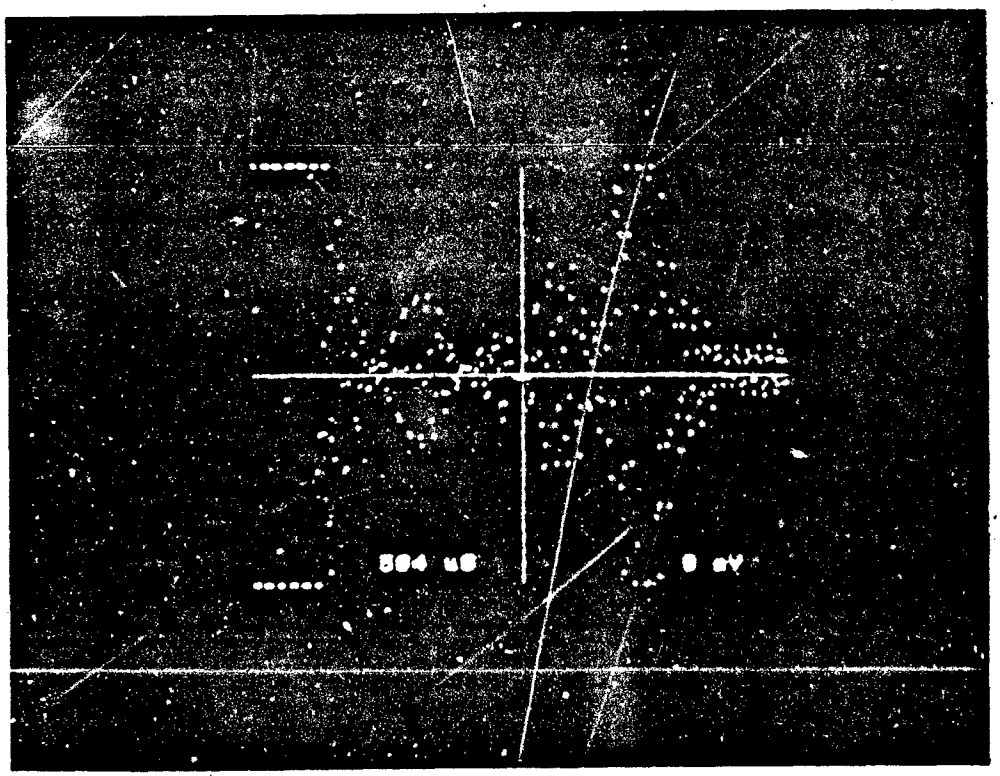

Figure 4.13. Measurement 5 at X = 48.8 cm.

$$T = 0.0450\ X^2 - 0.213\ X + 407$$

and the form for the reflections from the top of the sand is

$$T = 0.0463\ X^2 + 0.562\ X + 339$$

The incident angle for determining the ray parameter was 33.4 degrees so that the ray parameter P was $3.70 \times 10^{-6}$.

The ray parameter analysis gave 9.59 cm for $\Delta X$ and 71.5 μs for $\Delta T$; therefore, the sand layer depth was computed to be 4.58 cm--about six percent below the actual value. The calculated value for the sound speed in the sand layer was 1904 m/s which was significantly higher than any other of the determinations.

B. OVERALL RESULTS

In all, seven experiments were performed but the data from two of the experiments was not good enough to analyze. The other five experiments have been reported above and, except for number 5, the results were quite consistent with reasonable errors.

Table VI gives a summary of the results of the five experiments that were analyzed and compares the results of the $T^2$-$X^2$ method and the ray parameter method. The average error in determining the depth of the layer was 3.5 percent so this measurement can be done effectively; however, the

TABLE VI

Summary of Brief Results

| | MEASUREMENT CONTENT | 1 | 2 | 3 | 4 | 5 |
|---|---|---|---|---|---|---|
| Layer Depth (cm) | ACTUAL | 3.5(+.05) | 3.3(+.1) | 2.3(+.1) | 1.8(+.1) | 5.0(+.1) |
| | EXPERIMENTAL | 3.56 | 3.73 | 2.42 | 1.74 | 4.58 |
| | ERROR (%) | 0.3 | 9.7 | 0.8 | 0.0 | 6.5 |
| Speed of Sound (m/sec) | $T^2$-$X^2$ METHOD | 1662 | 1647 | 1649 | 1582 | 1577 |
| | RAY PARAMETER | 1791 | 1474 | 1578 | 1647 | 1904 |
| | DIFFERENCE | 163 | 154 | 49.6 | 18.9 | 275.9 |
| | ERROR (%) | 10.0 | 9.5 | 3.0 | 1.2 | 16.9 |

error in the sound speed calculation (for the sand layer) was fairly large (about 8 percent). Consequently, the sound speed determination is not quite as reliable.

In Table VI, the difference means the values between the average of the five $T^2$-$X^2$ results and the ray parameter method's value.

## V. DISCUSSIONS AND CONCLUSIONS

The objective of this research was to localize buried objects (e.g., thin aluminum plates) in water-saturated sand. In order to accomplish this objective, we needed to predict the sound speed and the depth of the overlying layer. The results are summarized in Table VII.

The average speed of sound by the $T^2$-$X^2$ method is 1472 m/sec for the direct wave, 1446 m/sec for the bottom reflected wave, 1623 m/sec for the wave through the sand.

Comparing the above sound speeds with the value given by Reference 3 (1481 m/sec at 20 °C), we had 0.6% error in the direct wave speed and 2.3% error in the bottom reflected wave speed.

Reference 3 gives the sound speeds 1540 m/sec for coarse silt and 1730 m/sec for quartz sand. The sand used in this experiment is #30 mesh sand (washed, kilndried and graded) and the measured sound speed is 1623 m/sec.

We used linear regression for finding the speed of sound with the $T^2$-$X^2$ method. Since most correlation values of the linear regression are over 95%, the $T^2$-$X^2$ method is reasonable for determining the speed of sound.

By using the ray parameter method, we determined $\Delta X$, $\Delta T$ and $\Delta z$. The average error between the actual layer's depth and the computed depth is 3.5%. The error range is between

TABLE VII

The Detailed Results of Total Experiment

| | DETAILS | | MEASUREMENT | 1 | 2 | 3 | 4 | 5 |
|---|---|---|---|---|---|---|---|---|
| | | | ACTUAL LAYER DEPTH (cm) | 3.5(±.05) | 3.3(±.1) | 2.3(±.1) | 1.8(±.1) | 5.0(±.1) |
| The $T^2-X^2$ Method | SPEED OF SOUND (m/sec) & LINEAR CORRELATION (%) | S | | 98.3 | 94.3 | 95.2 | 99.7 | 99.9 |
| | | | | 1661 | 1647 | 1649 | 1582 | 1577 |
| | | B | | 99.4 | 99.6 | 99.9 | 99.7 | 100 |
| | | | | 1416 | 1419 | 1471 | 1458 | 1468 |
| | | D | | 99.8 | 99.9 | 99.8 | 99.9 | 100 |
| | | | | 1463 | 1437 | 1510 | 1461 | 1488 |
| The Ray Parameter Method | | | P ($10^{-6}$ Sec/m) | 3.32 | 3.69 | 3.00 | 5.30 | 3.70 |
| | | | ΔX (cm) | 5.47 | 3.87 | 2.53 | 5.8 | 9.59 |
| | | | ΔT (μsec) | 51.4 | 54.0 | 33.9 | 40.4 | 71.5 |
| | | | Δz (cm) | 3.56 | 3.73 | 2.42 | 1.74 | 4.58 |
| | | | ERROR (%)[1] | 0.3 | 9.7 | 0.8 | 0.0 | 6.5 |
| | | | $c_1$ DIFFERENCE[2] (m/sec) | 163 | 154 | 50 | 19 | 276 |
| | | | ERROR (%)[3] | 10.0 | 9.5 | 3.0 | 1.2 | 16.9 |

# Average error of measuring Δz = 3.5%

# Average error of $c_1$ difference = 8.1%

[1] This error is the value when comparing the experimental Δz with actual layer's depth.

[2] $c_1$ difference is the difference between $c_1$ of $T^2-X^2$ and the value of the ray parameter method.

[3] This error is the value when comparing the $c_1$ difference with the average value of $T^2-X^2$.

0% and 9.7%. The ray parameter method is one of the most useful for finding an unknown layer's depth. But, the average error of $c_1$ between the $T^2$-$X^2$ and the ray parameter methods is relatively high (8.1%).

In every measurement the direct wave's speed of sound is always faster than that of the bottom reflected wave. These values should be the same because both are measures of the sound speed in water. This discrepancy is probably a result of the difficulty in determining the true horizontal distance between the acoustic center of the projector and the hydrophone for different angles of the projector. In some cases, the difference in $c_1$ between the $T^2$-$X^2$ and the ray parameter methods is over 10%. This may result from the choice of curve-fit for the T-X data. We tried several ways to find the best curve fit, but the computed results were quite different from the expected ones except for those from parabolic fit.

We had some limitations on the measurements because of the use of a small tank. In particular, there were interfering reflections. So, some of the signals arrive at the same time. That made the analysis of the layer speed of sound and depth very difficult. Also, the pulse length was too long to be able to resolve the thin layer. Projector ringing limits the pulse length so that it cannot be made shorter than a certain duration. Because of these problems, this experiment would be easier to do in a larger body of water.

If we do this experiment in the ocean instead of small water tank, then identifying the wave signals is much easier because of less multipath interference. In the ocean, we can try ASPER (airgun sonobuoy precision echo recorder) developed by the Hawaii Institute of Geophysics as one of the recommended methods [Ref. 1].

## LIST OF REFERENCES


1. Maynard, G.L., G.H. Sutton, D.M. Hussong and L.W. Kroenke, "The Seismic Wide Angle Reflection Method in the Study of Ocean Sediment Velocity Structure," Physics of Sound in Marine Sediments, Plenum Press, Lloyd Hampton, ed., 1974.

2. Bryan, George M., "Sonobuoy Measurements in Thin Layers," Physics of Sound in Marine Sediments, Plenum Press, Lloyd Hampton, ed., 1974.

3. Kinsler, L.E., A.R. Frey, A.B. Coppens, and J.V. Sanders, Fundamentals of Acoustics, pp. 427-429, third edition, John Wiley & Sons, 1982.

4. Bardin, J.L. and J.W. Whitely, Acoustic Reflection and Transmission Characterisics for Thin Plates, Applied Research Laboratories, The University of Texas at Austin, March, 1975.

5. Brekhovskikh, L, and Yu. Lysannov, Fundamentals of Ocean Acoustics, pp. 1-6, Springer Series in Eltrophysics 8, 1982.

6. Stephens, R.W.B., Underwater Acoustics, pp. 135-138, Wiley-Interscience, 1970.

7. Bobber, Robert J., Underwater Electroacoustic Measurements, pp. 134-148, Naval Research Laboratory, Washington, D.C., 1970.

## INITIAL DISTRIBUTION LIST

| | | No. Copies |
|---|---|---|
| 1. | Defense Technical Information Center<br>Cameron Station<br>Alexandria, Virginia 22304-6145 | 2 |
| 2. | Library, Code 0142<br>Naval Postgraduate School<br>Monterey, California 93943-5100 | 2 |
| 3. | Prof. Suk Wang Yoon, Code 61Yo<br>Naval Postgraduate School<br>Monterey, California 93943-5100 | 5 |
| 4. | Prof. Thomas B. Gabrielson, Code 61Gt<br>Naval Postgraduate School<br>Monterey, California 93943-5100 | 2 |
| 5. | Department Chairman, Code 61<br>Department of Physics<br>Naval Postgraduate School<br>Monterey, California 93943-5100 | 2 |
| 6. | Gwan-Sik Bang<br>5 dong 404 ho Cheolsan Arpartment<br>cheolsan 4 dong Kwang Myeong City<br>Kyeong gi do Republic of Korea | 8 |
| 7. | Major Chang-Ho Yim<br>SMC #2425<br>Naval Postgraduate School<br>Monterey, California 93943-5100 | 1 |
| 8. | Cpt In-Seop Park<br>SMC #2886<br>Naval Postgraduate School<br>Monterey, California 93943-5100 | 1 |
| 9. | Major Yeon Duck Koo<br>SMC #2750<br>Naval Postgraduate School<br>Monterey, California 93943-5100 | 1 |
| 10. | Major Sang Chu Yoon<br>SMC #2750<br>Naval Postgraduate School<br>Monterey, California 93943-5100 | 1 |

11. Lt. Young soo Kim 1
SMC #2681
Naval Postgraduate School
Monterey, California 93943-5100

12. Lt Pal Man Park 1
SMC #2400
Naval Postgraduate School
Monterey, California 93943-5100

END

FILMED

9-85

DTIC